Nanoscale

Accepted Manuscript

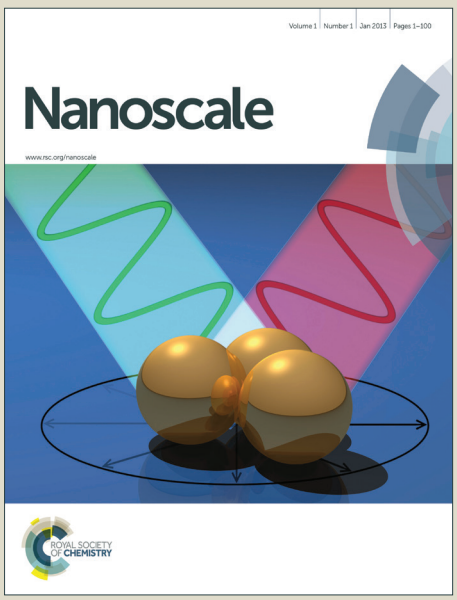

ROYAL SOCIETY OF CHEMISTRY

www.rsc.org/nanoscale

Single-excitation dual-color coherent lasing by tuning resonance energy transfer process in porous structured nanowires

Zhaona Wang[1,*], Xiaoyu Shi[1], Ruomeng Yu[2], Sujun Wei[1], Qing Chang[1], Yanrong Wang[1], Dahe Liu[1,*] and Zhong Lin Wang[2,3]

[1]Applied Optics Beijing Area Major Laboratory, Department of Physics , Beijing Normal University, Beijing, China, 100875

[2]School of Materials Science and Engineering, Georgia Institute of Technology, Atlanta, Georgia 30332-0245, USA

[3]Beijing Institute of Nanoenergy and Nanosystems, Chinese Academy of Sciences, Beijing, China, 100083

†Electronic supplementary information (ESI) available: Materials and methods, Fig. S1–6.

*Email: zhnwang@bnu.edu.cn and dhliu@bnu.edu.cn

ABSTRACT

Single-excitation dual-color coherent lasing was firstly achieved in a binary-dye mixed random system by suspending scatterer of gold-silver porous nanowires with plenty of nanogaps, which can greatly enhance the local electromagnetic field in the visible range and guarantee a low threshold and high Q factor (>10,000) operator for simultaneously dual-color lasing. By tuning the resonance energy transfer process in the stimulated emission process, triple output modes: single chartreuse lasing, chartreuse & red dual-color lasing, and single red coherent lasing can be easily obtained. The demonstrated triple-mode coherent random lasing introduces a new approach of designing multi-function micro-optoelectronic devices for multi-color speckle-free imaging and interference.

Keywords: *coherent lasing; resonance energy transfer; Au-Ag bimetallic porous*

nanowire; surface plasmon resonance

1. Introduction

Multi-color coherent laser sources achieved with low cost through simple processes are highly demanded in micro optoelectronics, imaging and related fields.[1-4] Among the existing laser systems, random laser is considered as one of the most prospective approaches with easy process for its small size and resonance cavity-free configurations,[5-9] low spatial coherent property suit for speckle-avoided imaging.[10] Generally, scatterers in a random laser system play an essential role in extending the optical path and forming the loop for optical feedbacks. When pumped by pulsed lasers, random lasing systems may present two types of feedbacks: incoherent feedback[11-14] with peaks of several nanometers in linewidth and coherent feedback[15-21] with spikes narrower than 1 nm in linewidth. Tremendous research efforts have been devoted in developing low-threshold random lasers with single color emissions.[7, 8, 11-13, 15, 16, 18] However, single excitation-induced multi-color random lasing systems have long been desired except for few reports,[14, 22, 23] which all supplied incoherent emissions and can't suit for the requirements of the coherent property. Coherent random lasers with multi-color emissions through single excitation are therefore necessary for future integrated and multi-function applications in the field of multi-color speckle-free imaging,[10] interference, secure encoding and quantum optics.

Two major challenges are hindering the achievement of simultaneous multi-color coherent random lasing through single-excitation. The first is finding a dye system

possessing two or more emission bands with easily-tuned emission efficiency at different wavelengths. R6G and oxazine mixed binary-dye system is chosen to overcome this challenge by utilizing the well-investigated resonance energy transfer (RET) process[24-26] between these two dyes, considering the absorption band of oxazine partially overlapping with the emission band of R6G. To obtain the dual-color lasing, too large and too small energy transfer efficiency should be avoided. And the average distance of the molecules should not be smaller than Förster distance too many for moderate energy transfer efficiency, which is different from the other reports.[22, 23, 27, 28] Usually, metal nanoparticles with a regular shape are used to enhance the local electromagnetic field (LEF) by coinciding their narrow plasmonic resonance (PR) peaks with single random lasing peak in most cases.[12, 13, 29, 30] But the narrow PR peak and the limited LEF enhancement effect are not good for achieving multi-color random lasing. Thus the second challenge is synthesizing nanostructures as scatterers not only possessing broad band PR spectrum but also providing enough strong LEF enhancement for random lasing at different wavelengths. Here, gold-silver (Au-Ag) bimetallic porous nanowires (NWs) synthesized through low temperature solution process are employed considering their broad band of PR spectrum over the whole visible range. More importantly, the porous NWs have plenty of nanogaps, which introduce large LEF enhancement factors for the electromagnetic waves at different wavelength. [27]

In this work, we achieved coherent dual-color random lasing based on a R6G/oxazine mixed binary-dye system through controlling the RET process under the

low pump power densities. The triple-output-mode: chartreuse lasing, chartreuse & red dual-color lasing, the red lasing is derived by adjusting the mixing ratio between two dyes. The linewidths of lasing modes are less than 0.1 nm. Au-Ag porous NWs with abundant nanogaps are merged into this system as scatterers to significantly enhance the LEFs in visible range and lower the operation threshold of simultaneous multi-color lasing.

2. Results and Discussions

The molecular formula structures of R6G (the donor) and oxazine (the acceptor) are presented in Fig. 1a, along with the corresponding photoluminescence (PL) and absorption spectra shown in Fig. 1b. The PL spectra peak of dye R6G (dash dot orange curve) partially overlaps with the absorption band of oxazine (doted red curve) at 577 nm to efficiently built up the RET between them[27] with R6G as the donor and oxazine as the acceptor. Considering the incomplete overlap between the emission band of donors and the absorption band of acceptors and large average distances of molecules, only part of the donors' energies are transferred to the acceptors with the rest remained for stimulated emissions as indicated in Fig. 1c for details. Upon absorbing the photon energy from a 532 nm pumping pulses, the donor (R6G) dye molecules are excited to the energy state of $R_{excited}$, followed by a vibrational relaxation to the energy state of $R_{vibronic}$ as shown in Fig. 1c. Some R6G molecules in the excited states decay to lower energy states *via* either nonradiative decay at a rate of γ_R or radiative decay at a rate of Γ_R with emissions at ~574 nm. Other excited R6G

molecules resonantly and nonradiatively transfer electronic energies to the oxazine dye molecules through the RET process to excite the acceptor molecules. On the other hand, acceptors are excited by absorbing energies from either the 532 nm pumping source or excited R6G molecules through RET process and then decay to the ground states. Emissions at around 638 nm are thus observed from decays in radiative manners. Based on this physical mechanism, dual-color output is obtained from mixing R6G/oxazine binary-dye system under single excitation conditions through the moderate RET process.

Au-Ag bimetallic porous NWs are fabricated by hydrothermal method under low temperature as reported previously (Methods).[19, 27] The nanostructures of as-synthesized Au-Ag NWs are characterized by scanning electron microscope (SEM) as shown in Figs. 1d and S1 (Supporting Information), presenting abundant nanogaps on porous NWs with an averaged diameter of 80 nm and length of 10 μm. This unique porous structure leads to a continuous extinction spectrum (inset of Fig. 1d) that covers the PL peak of mixed R6G/oxazine binary-dye system (brown curve in Fig. 1b). Au-Ag porous nanostructures synthesized in this manner possess nano-gaps that can be easily fabricated and tuned in density compared with other broad extinction spectrum materials.[31] Finite element analysis is conducted to investigate the electromagnetic field enhancements by nanogaps in Au-Ag porous nanostructures as shown in Fig. S2 (Supporting Information). Large field enhancement factors of 100 at 574 nm and 200 at 638 nm are derived for Au-Ag NWs with nanogaps in comparisons with those obtained from pure Ag NWs (2.4 at 574 nm and 2.3 at 638 nm), indicating

the capability of Au-Ag NWs to provide simultaneously strong feedback and gain channels as light amplifications[27] for coherent lasing process. Finally, donor dye R6G and acceptor dye oxazine are added to the Au-Ag NWs suspension at certain concentration of 7.56×10^7/ml (unless otherwise specified) to build the RET random laser systems.

The high resolution emission spectra under 532 nm pump pulses with different power densities above the thresholds derived from the Au-Ag NWs-based binary-dye systems with R6G and oxazine at concentrations of 0.43 mg/ml and 0.008 mg/ml (i.e. molecular ratio between R6G and oxazine is α=44.4, and the average distance of the molecules is larger than 10 nm), respectively, are presented in Fig. 2a. Under the pump power density of 1.07 MW/cm^2 (red curves in Fig. 2a), coherent random lasing characterized by the sub-nanometer spikes is observed at ~573 nm as reported in other random systems.[15-21] These results show that a small portion of energy is transferred from R6G to the gain material oxazine, which makes the gain larger than the loss in some loops for R6G but not for oxazine due to extended optical paths. Under a moderated value of 1.33 MW/cm^2 pump power density, dual-band coherent random lasing characterized by two series of sharp spikes at the center wavelength of 573 nm and 636 nm are simultaneously observed (photograph presented in Fig. 2b) as indicated by blue curves in Fig. 2a. This implies that the coherent lasing resonances from the two gain materials are built up simultaneously under single-wavelength pumping laser, which is derived from the optical gain based on moderated RET and the great enhancement of LEF induced by abundant nanogaps in the Au-Ag porous

NWs (Figs. S2c and d, Supporting Information). Similar dual-color coherent random lasing can be observed under a pump power density of 1.67 MW/cm^2 (olive curves in Fig. 2a).

To demonstrate the linewidths of the lasing modes, the enlarged view of two emission bands in Fig. 2a are shown in Figs. 2c and 2d. Multiple lasing modes are clearly observed with random positions and with the linewidths of less than 0.1 nm. These spikes present random lasing from different feedback cavities.[32] Furthermore, the full width at half maximum (FWHM) of two lasing lines at 574.14 nm and 636.10 nm in olive in Fig. 3c and 3d are measured and shown in Fig. S3a and S3b (Supporting Information), respectively. The FWHM of lasing lines at 574.14 nm and 636.10 nm is about 0.05 nm and 0.06 nm, the quality (Q) factor, defined as λpeak /FWHM, is about ~11,000 and ~10,000, respectively. High Q factors are comparable to other lasing systems with additional feedback.[33, 34]

The corresponding maximal emission intensity under each pump power densities and linewidths of random lasing modes derived from the emission band of R6G and that of oxazine are analyzed and summarized in Figs. 2e and f, respectively. The threshold is 0.87 MW/cm^2 (about 4.3 mJ) for coherent random lasing from R6G and 1.01 MW/cm^2 (about 5.1 mJ) for coherent lasing from oxazine. Compared with the performance of Au-Ag NWs-based systems with single R6G in the concentrate of C_{R6G} = 0.43 mg/ml (Fig. S4, Supporting Information), the threshold of the random lasing from R6G is increased from 0.51 MW/cm^2 to 0.87 MW/cm^2 attributing to the RET process from R6G to oxazine. It should be emphasized that the thresholds of the

dual-color coherent random lasing from binary-dye random system are competitive and even lower than those derived from single-dye random systems for either incoherent[13] (about 15 mJ) or coherent[18] (>1.5 MW/cm^2) lasing.

To confirm the essential role played by the RET process between R6G and oxazine during the coherent dual-color random lasing emissions, several control experiments are conducted for verification purposes. First, the emission spectrum of an Au-Ag NWs based single oxazine dye system (oxazine concentration = 0.008 mg/ml) pumped by 532 nm pulsed laser is presented in Fig. 3a, showing a broad spontaneous emission spectrum with a linewidth of 35 nm without sharp spikes under the pump power density ranging from 1.33 to 6.53 MW/cm^2, along with a faint red color emission photograph (Fig. 3b). These results confirm that no coherent random lasing is derived from single oxazine dye systems under 532 nm pumping, since the photon energy is hardly absorbed due to a huge deviation from the absorption peak (about 610 nm) of oxazine. Furthermore, to investigate the energy transfer efficiency of RET in the stimulate emission process, 574 nm (same to the emission peak of R6G as shown in Fig. 3c) pulses are applied as pumping sources for Au-Ag NWs based single oxazine dye systems as well. Under the same concentration of oxazine (0.008 mg/ml) to that the in dual-color random laser, only broad PL spectra are observed under the pump power densities between 1.23 and 2.53 MW/cm^2 (Fig. S5a, Supporting Information), indicating no random lasing is derived under this condition. Until oxazine concentrations increase larger than 0.1 mg/ml, coherent random lasing is derived when fixing the pumping power density of 574 nm nanosecond pulses at

1.33 MW/cm^2 (Fig. S5b, Supporting Information). Compared with R6G/oxazine binary-dye systems that emit coherent lasing at extremely low oxazine concentration of 0.008 mg/ml, it is concluded that RET process significantly reduce the amount of dye materials demanded about 12 times to develop economic and high performance random lasers.

The significance of Au-Ag porous NWs is carefully studied by comparing the emission characteristic of Ag NWs-based binary-dye random systems (red curves) and pure binary-dye system (black curves) as shown in Fig. 3d. The spectra show that no coherent emission is obtained from random systems either with Ag NWs as scatterers (red curves) or without any scatterers (black curves) pumped by a 532 nm pulsed laser at a power density of 1.01 MW/cm^2. These results clearly indicate that Au-Ag porous NWs are necessary for the coherent random lasing by providing strong feedback and gain channels during the RET process.[19] The unique surface plasmon resonate property that covers the whole visible range make Au-Ag NWs an ideal scatterer for multi-wavelength random lasers. It should be stated that for pure binary-dye system, the red output light is stronger than the yellow light, while yellow is stronger than red light in the Ag NWs-based system, attributing to the Ag NWs can supply larger LEF enhancement at 574 nm chartreuse than that at 638 nm red as shown in Supplementary Figs. S2a and S2b.

The output characteristics of the binary-dye random lasing systems can be effectively tuned by adjusting the mixing ratio between R6G and oxazine as shown in Figs. 4a and b. When keeping the concentration of R6G as 0.43 mg/ml (related to the

average distance among molecules about 12.3 nm) and varying the concentration of oxazine from 0.004 mg/ml (the bottom) through 0.007 mg/ml (the middle) to 0.01 mg/ml (the top), the lasing output transits from chartreuse coherent lasing emitted from R6G (the bottom) through the simultaneous chartreuse & red coherent lasing (the middle) to red coherent lasing from oxazine (the top), as shown in Fig. 4a. The transitions among three emission modes are also obtained by changing the concentration of R6G from 0.3 mg/ml to 0.7 mg/ml while keeping the oxazine concentration of 0.008 mg/ml fixed as shown in Fig. 4b. The output coherent lasing modes always have the narrow linewidth of less than 0.1 nm (see inset in Fig.4) and high Q factor. These results indicate that three coherent lasing output modes are switched by varying the mixing ratio between R6G and oxazine dyes.

The working mechanism behind the capability of switching output lasing modes through tuning the mixing ratio between R6G and oxazine is explained by considering the tunable RET efficiency during the emissions in porous bimetallic nanowires as shown in Fig. 5. When moderate R6G molecules in the random system (i. e. the moderate average distance between donors and acceptors) meet a few oxazine molecules, R6G molecules absorb 532 nm photons and are thus excited to higher energy states. The excited R6G molecules transfer a small portion of energy to oxazine molecules with plenty energy remained to build up the coherent feedback in nanogaps, which can greatly enhance the LEF and provide larger gain. Oxazine molecules obtain the gain from 532 nm pump source and/or the donor of R6G is smaller than the loss in the loops and coherent feedback cannot be formed. Only

chartreuse coherent lasing emission is derived from the RET-based random system under this condition as shown in Fig. 5a. As increasing the amount of oxazine to a moderate level, the excited R6G molecules can guarantee enough gain to surpass optical losses in the feedback loops (in yellow dot line), and provide sufficient energy to excite oxazine molecules in the meanwhile, leading to the chartreuse & red dual-color coherent laser emitting as shown in Fig. 5b. However, by further increasing oxazine, a huge portion of energy is transferred from R6G to oxazine, leaving insufficient energy for lasing resonance in R6G. In this case, only oxazine has enough gain for stimulated radiation, emitting coherent lasing only in red color as shown in Fig. 5c.

A general guidance of the relationship between lasing output mode and mixing ratio of R6G/oxazine is summarized based on the discussions presented above. When the concentration of R6G is fixed at 0.43 mg/ml, dual-color random lasing is derived by keeping the concentration of oxazine in the range of [0.007, 0.009] mg/ml. With oxazine concentration fixed at 0.008 mg/ml, R6G concentration in the range of [0.4, 0.6] mg/ml provides emissions of multi-colors. Besides, it is found that the relationship between output modes and mixing ratio depends on the concentration of the scatterers as well. By decreasing the concentration of Au-Ag NWs to 3.78×10^{7}/ml, similar controlling phenomena with three emission modes are observed at lower dye concentrations as presented in Fig. S6. Detailed discussions are found in Supporting Information.

These results indicate that a white light random laser can be achieved by mixing

various dyes with different emissions wavelengths in a proper concentrate as well as ratio. Therefore, the energy transfer process between the dye molecules should be taken into account in designing multi-color and/or multi-function random lasers.

3. Conclusions

By controlling the RET process when the average distance of the donors and acceptors is larger than 10 nm, coherent dual-color random lasing is achieved based on a R6G/oxazine mixed binary-dye system. A triple-mode random laser switching among the chartreuse lasing, the chartreuse & red dual-color lasing, the red lasing is derived based on tuning and controlling the process of RETs between R6G and oxazine. And transitions among these three lasing modes are obtained by easily adjusting the mixing ratio between two dyes. Au-Ag porous NWs with abundant nano-gaps are merged into this system as scatterer to significantly enhance the LEFs in visible range and lower the operation threshold of simultaneous multi-color lasing. These results indicate a new economical approach for fabricating multi-color coherent random lasers and present a prospective direction for future multi-function micro-optoelectronic devices, also supply a new way for learning the mechanism of RET in the coherent feedback and in porous structured nanowires.

Methods:

Preparation of binary-dye random lasing systems*:* First, Ag NWs with diameter of 80 nm and length of 10 μm (Fig. S1a, Supporting Information) are synthesized by polyvinylpyrrolidone-assisted reaction in ethylene glycol as reported previously.[35, 36] Then the purified Ag NWs dispersion in ethanol with a concentration of 7.56×10^7/ml

are exposed to $HAuCl_4$ solution with a molar ratio between $HAuCl_4$ and Ag as $\gamma_M = M_{Au}:M_{Ag} = 0.126$ for the galvanic replacement reaction,[19, 37] forming the porous bimetal nanostructures with nano-gaps as shown in Figs. 1d and S1b (Supporting Information). Finally, donor dye R6G and acceptor dye oxazine are added to the Au-Ag NWs suspension at certain concentrations to build the resonance-energy-transfer random laser systems.

Materials Characterization: The microscopic structures of Au-Ag NWs are characterized by scanning electron microscope (SEM) (Hitachi SU8010).

Optical measurements*:* The mixed suspension prepared above is collected in a cuvette with a length of 20 mm, width of 10 mm, and height of 45 mm. The binary-dye system is then vertically pumped by a Q-switched frequency-doubled Nd:YAG pulsed laser (Continuum model PowerLite Precision 8000) with a wavelength of 532 nm, pulse duration of 8 ns, repetition rate of 10 Hz, and the out-beam diameter of 8 mm. The 574 nm nanosecond pulsed laser was generated by Optical Parametric Oscillators pumped by Q-switched Nd:YAG pulsed laser. The emission spectra of the RET random lasing systems are collected horizontally by a Princeton Instruments spectrometer (Acton SP2750) with high resolution of 0.01 nm or an optical fiber spectrometer (Ocean Optics model Maya Pro 2000 with a spectral resolution of 0.4 nm). To determine the thresholds of dual-color random lasing, the chartreuse emission and red emission were separately tracked for several seconds under each pump power density by using screen recorder. Then the maximal intensity was obtained to plot the threshold curves. Considering the randomly distributed sharp

spikes meaning the lasing oscillations, the linewidth is taken as 0.1 nm after coherent random lasing spikes appear in the emission spectra.

Acknowledgements

The National Natural Science Foundation of China (grant Nos. 11104016, 11074024, and 61275130), Beijing Higher Education Young Elite Teacher Project and the Fundamental Research Funds for the Central Universities are acknowledged for financial support.

References:

1. C. Dang, J. Lee, C. Breen, J. S. Steckel, S. Coe-Sullivan and A. Nurmikko, *Nat Nanotechnol*, 2012, **7**, 335-339.
2. A. L. Pan, W. C. Zhou, E. S. P. Leong, R. B. Liu, A. H. Chin, B. S. Zou and C. Z. Ning, *Nano Letters*, 2009, **9**, 784-788.
3. Z. C. Liu, L. J. Yin, H. Ning, Z. Y. Yang, L. M. Tong and C. Z. Ning, *Nano Letters*, 2013, **13**, 4945-4950.
4. X. P. Hu, G. Zhao, Z. Yan, X. Wang, Z. D. Gao, H. Liu, J. L. He and S. N. Zhu, *Optics Letters*, 2008, **33**, 408-410.
5. D. Wiersma, *Nature*, 2000, **406**, 132-133.
6. H. Cao, J. Y. Xu, D. Z. Zhang, S. Chang, S. T. Ho, E. W. Seelig, X. Liu and R. P. Chang, *Phys Rev Lett*, 2000, **84**, 5584-5587.
7. N. Bachelard, S. Gigan, X. Noblin and P. Sebbah, *Nat Phys*, 2014, **10**, 426-431.
8. H. E. Tureci, L. Ge, S. Rotter and A. D. Stone, *Science*, 2008, **320**, 643-646.
9. M. Leonetti, C. Conti and C. Lopez, *Nature Photonics*, 2011, **5**, 615-617.
10. B. Redding, M. A. Choma and H. Cao, *Nat Photonics*, 2012, **6**, 355-359.
11. R. Pierrat and R. Carminati, *Physical Review A*, 2007, **76**.
12. G. D. Dice, S. Mujumdar and A. Y. Elezzabi, *Appl Phys Lett*, 2005, **86**.
13. O. Popov, A. Zilbershtein and D. Davidov, *Appl Phys Lett*, 2006, **89**.
14. S. J. Chen, X. Y. Zhao, Y. R. Wang, J. W. Shi and D. H. Liu, *Appl Phys Lett*, 2012, **101**.
15. X. G. Meng, K. Fujita, S. Murai and K. Tanaka, *Physical Review A*, 2009, **79**.
16. H. Cao, J. Y. Y. Xu, Y. Ling, A. L. Burin, E. W. Seeling, X. Liu and R. P. H. Chang, *Ieee J Sel Top Quant*, 2003, **9**, 111-119.
17. H. Cao, *J Phys a-Math Gen*, 2005, **38**, 10497-10535.
18. Y. Y. Sun, Z. N. Wang, X. Y. Shi, Y. R. Wang, X. Y. Zhao, S. J. Chen, J. W. Shi, J. Zhou and D. H. Liu, *J Opt Soc Am B*, 2013, **30**, 2523-2528.
19. X. Y. Shi, Y. R. Wang, Z. N. Wang, Y. Y. Sun, D. H. Liu, Y. Y. Zhang, Q. W. Li and J. W. Shi, *Appl Phys Lett*, 2013, **103**.
20. Y. R. Wang, X. Y. Shi, Y. Y. Sun, R. Q. Zheng, S. J. Wei, J. W. Shi, Z. N. Wang and D. H. Liu, *Optics Letters*, 2014, **39**, 5-8.
21. S. X. Wang Z., Wei S., et al. , *Laser Phys Lett*, 2014, **11**, 095002
22. M. Ibisate, J. F. Galisteo-Lopez, V. Esteso and C. Lopez, *Advanced Optical Materials*, 2013, **1**, 651-656.
23. J. F. Galisteo-López, M. Ibisate and C. López, *The Journal of Physical Chemistry C*, 2014, **118**, 9665-9669.
24. V. V. Didenko, *Biotechniques*, 2002, **32**, 1012-1012.
25. P. R. Selvin, *Nat Struct Biol*, 2000, **7**, 730-734.
26. M. Berggren, A. Dodabalapur, R. E. Slusher and Z. Bao, *Nature*, 1997, **389**, 466-469.
27. X. Y. Shi, Y. R. Wang, Z. N. Wang, S. J. Wei, Y. Y. Sun, D. H. Liu, J. Zhou, Y. Y. Zhang and J. W. Shi, *Adv Opt Mater*, 2014, **2**, 88-93.
28. S. S. Vogel, C. Thaler and S. V. Koushik, *Science Signaling*, 2006, **2006**, re2.
29. O. Popov, A. Zilbershtein and D. Davidov, *Polym Advan Technol*, 2007, **18**, 751-755.

30. X. G. Meng, K. Fujita, Y. Moriguchi, Y. H. Zong and K. Tanaka, *Adv Opt Mater*, 2013, **1**, 573-580.
31. A. Aubry, D. Y. Lei, A. I. Fernandez-Dominguez, Y. Sonnefraud, S. A. Maier and J. B. Pendry, *Nano Letters*, 2010, **10**, 2574-2579.
32. H. Cao, J. Y. Xu, S. H. Chang and S. T. Ho, *Physical Review E*, 2000, **61**, 1985.
33. M. H. Kok, W. Lu, J. C. W. Lee, W. Y. Tam, G. K. Wong and C.-T. Chan, *Applied Physics Letters*, 2008, **92**, 151108-151108-151103.
34. S. Shinohara, T. Fukushima and T. Harayama, *Physical Review A*, 2008, **77**, 033807.
35. L. F. Gou, M. Chipara and J. M. Zaleski, *Chem Mater*, 2007, **19**, 1755-1760.
36. Y. G. Sun, B. Gates, B. Mayers and Y. N. Xia, *Nano Letters*, 2002, **2**, 165-168.
37. N. L. Netzer, C. Qiu, Y. Y. Zhang, C. K. Lin, L. F. Zhang, H. Fong and C. Y. Jiang, *Chem Commun*, 2011, **47**, 9606-9608.

Figure captions

Figure 1. Fundamentals of dual-color coherent random laser. (a) Molecular formula structure of R6G (the top) and oxazine (the bottom); (b) The absorption spectra (the dot line, C_{R6G} = 0.008 mg/ml) and the PL spectra (the dash dot line, C_{R6G} = 0.43 mg/ml) of R6G solution (in orange) and oxazine solution (in red, $C_{oxazine}$ = 0.008 mg/ml) in ethanol, and PL spectra (in brown, C_{R6G} = 0.43 mg/ml, $C_{oxazine}$ = 0.008 mg/ml) of the solution mixing R6G and oxazine; (c) Energy diagram for the resonance energy transfer in the donor R6G dye and the acceptor oxazine dye; $R_{excited}$ and $R_{vibronic}$ are the excited electronic states and the corresponding vibronic states of the donor R6G molecules, respectively. Similarly, O is used for acceptor, and δ is the transfer rate. (d) Scanning electron microscope (SEM) images of Au-Ag porous NWs, the inset shows the extinction spectra of the corresponding Au–Ag NWs dispersion in ethanol.

Figure 2. **Simultaneous dual-color coherent random lasing emission.** (a-d) High-resolution emission spectra (a), the corresponding photograph (b) and the enlarged view of chartreuse (c) and red (d) emission bands in Fig. 2a of the binary-dye RET random system with R6G in the concentration of 0.43 mg/ml, oxazine in the concentration of 0.008 mg/ml and Au-Ag NWs in the concentration of 7.56×10^7/ml, pumped by 532 nm nanosecond pulsed lasers. The inset of (a) schematically shows the fundamental for dual-color coherent lasing. (e,f) The thresholds behavior of random lasing from R6G (e) and lasing from oxazine (f) with

respect to linewidth and output intensity of the binary-dye RET random system.

Figure 3. Significance of RET process and Au-Ag porous NWs. (a) Emission spectra of Au-Ag NWs based single-dye oxazine systems with oxazine concentration of $C_{Oxazine}$ = 0.008 mg/ml, pumped by 532 nm pulse laser under different pump power densities; (b) The corresponding photograph of (a). (c) Emission spectra of R6G with concentration of C_{R6G} = 0.43 mg/ml (orange curve) pumped by 532 nm pulses at the power density of 1.33 MW/cm^2; the absorption spectra of the R6G/oxazine binary-dye systems with C_{R6G} = 0.043 mg/ml and $C_{Oxazine}$ = 0.0008 mg/ml (black curve), the green dashed line is a label of 532 nm pumping laser; (d) Emission spectra of R6G/oxazine binary-dye systems with Ag NWs as scatterer (red curve) and without scatterer (black curve), pumped by 532 nm laser at 1.33 MW/cm^2 power density. The spectra are obtained from the optical fiber spectrometer with a spectral resolution of 0.4 nm.

Figure 4. **Transitions among three emission modes by tuning the mixing ratio between R6G and oxazine**. Single red coherent lasing (the top row), dual-color chartreuse & red coherent lasing (the second row), and single chartreuse coherent lasing (the bottom row) from binary-dye RET random system by changing the concentration of oxazine at C_{R6G}=0.43 mg/ml (a), and the concentration of R6G at $C_{Oxazine}$= 0.008 mg/ml (b), pumped by 532 nm pulsed laser with power density of 1.33 MW/cm^2.

Figure 5. **Schematic illustration of the mechanism of transitions among three emission modes upon tuning the mixing ratio between two dyes.** (a) When moderate R6G molecules and few oxazine molecules in nanogaps, only chartreuse light can get enough gain in some scattering loops (in yellow dot line) and achieve stimulated emission. (b) When moderate R6G molecules with moderate oxazine molecules in the dispersion, chartreuse light and red light can simultaneously form coherent feedback and lasing output. (c) When moderate R6G molecules meeting excess oxazine molecules, enough energy was transferred from R6G to oxazine molecules, leading to the weak emission from R6G and only red coherent lasing from the random system.

Figure 1

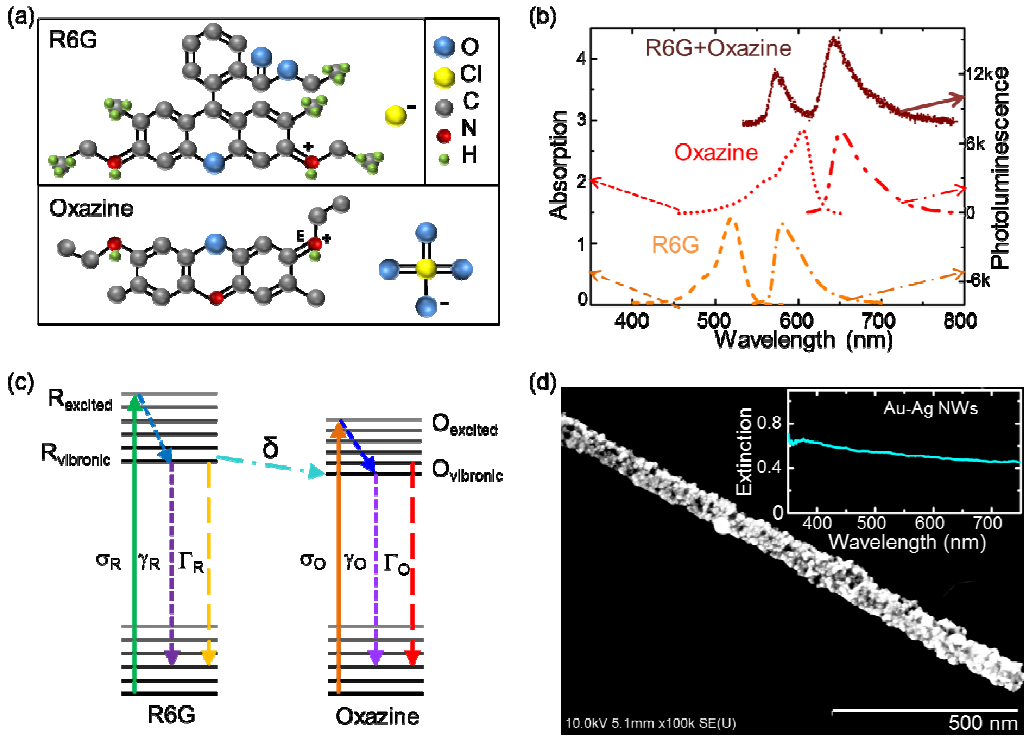

Figure 2

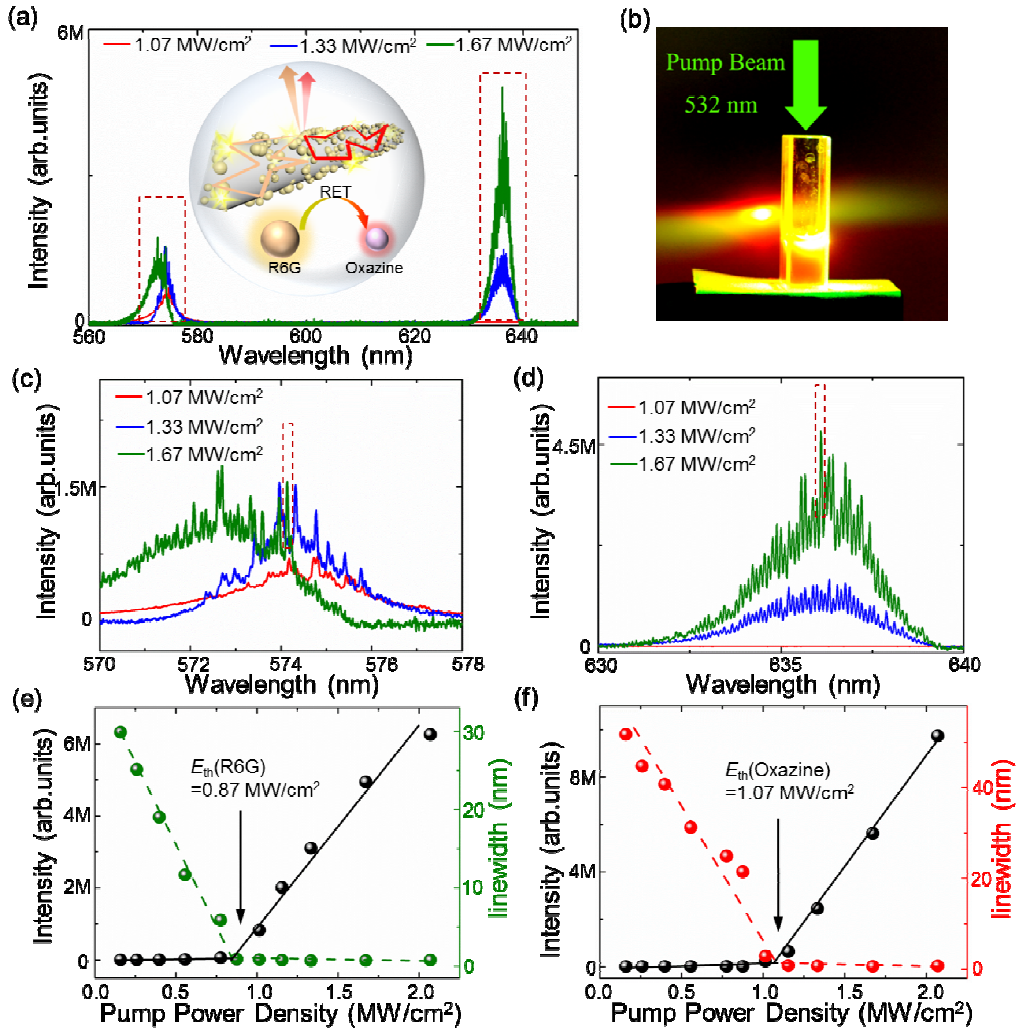

Figure 3

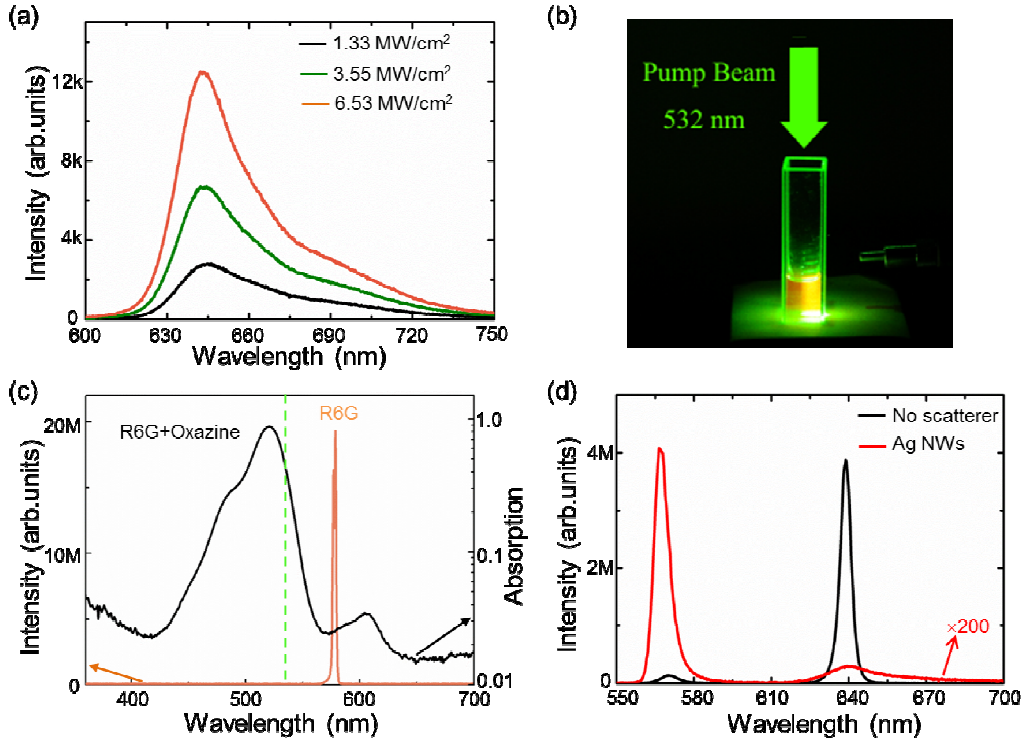

Figure 4

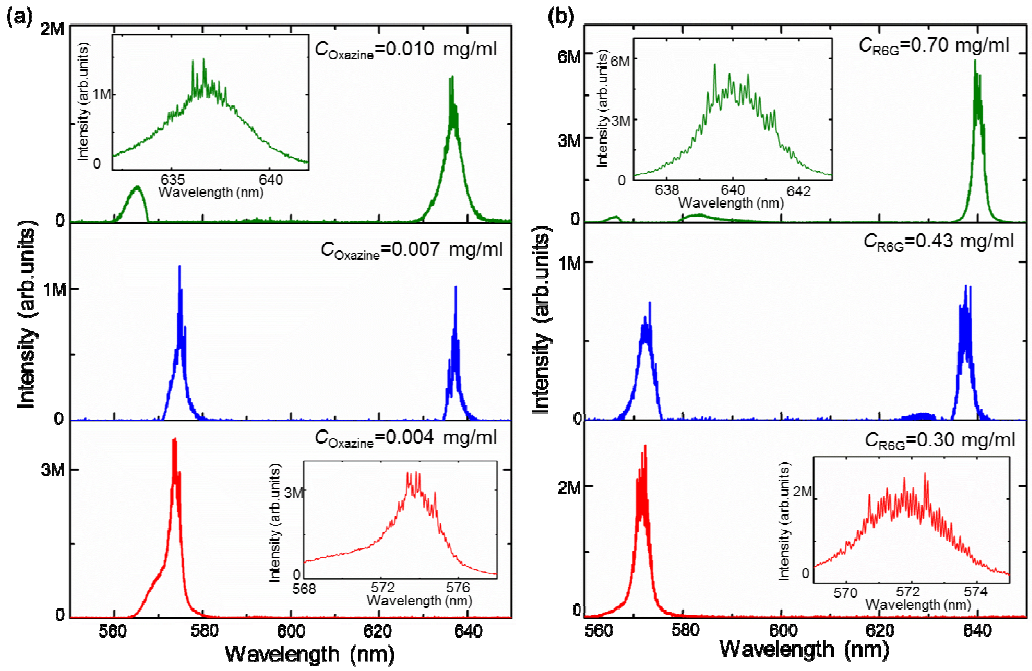

Figure 5